cogent engineering

Cogent Engineering

Taylor & Francis
Taylor & Francis Group

ISSN: (Print) 2331-1916 (Online) Journal homepage: https://www.tandfonline.com/loi/oaen20

Investigation of temperature and pressure effects on thermodynamic parameters of intermetallic alloy in EXAFS

Nguyen Ba Duc |

To cite this article: Nguyen Ba Duc | (2020) Investigation of temperature and pressure effects on thermodynamic parameters of intermetallic alloy in EXAFS, Cogent Engineering, 7:1, 1759184

To link to this article: https://doi.org/10.1080/23311916.2020.1759184

Published online: 04 May 2020.

Duc, *Cogent Engineering* (2020), 7: 1759184
https://doi.org/10.1080/23311916.2020.1759184

cogent engineering

MATERIALS ENGINEERING | RESEARCH ARTICLE

Investigation of temperature and pressure effects on thermodynamic parameters of intermetallic alloy in EXAFS

Nguyen Ba Duc[1]*

Received: 07 January 2020
Accepted: 16 April 2020

*Corresponding author: Nguyen Ba Duc, Faculty of Physics, Tan Trao University, Tuyen Quang, Viet Nam
E-mail: ducnb@daihoctantrao.edu.vn

Reviewing editor:
Blaza Stojanovic, University of Kragujevac, Faculty of Engineering, Serbia

Additional information is available at the end of the article

Abstract: This work advances the anharmonic correlated Einstein model to investigate how pressure and temperature affect the Debye–Waller factor and thermodynamic parameters of an intermetallic alloy. By using the anharmonic correlated Einstein model in extended X-ray absorption fine structure (EXAFS) theory, analytical expressions are derived for the effective spring constant, EXAFS cumulants, the anharmonic factor, and the thermal expansion coefficient at high temperature and pressure. The results show that both the anharmonicity of the thermal atomic vibration and the effects of pressure are essential for the thermodynamic parameters and the EXAFS Debye–Waller factor, as well as showing that the anharmonic contributions are important in the EXAFS spectrum. Numerical calculations of these thermodynamic quantities are performed for pure Cu and Ag and for CuAg72 alloy, and the results are consistent with those obtained experimentally and from other theories.

Subjects: Metals & Alloys;; Theoretical Physics;; Condensed Matter Physics;;

Keywords: Anharmonic; cumulant; Debye–Waller factor; intermetallic alloy; pressure

ABOUT THE AUTHOR

Duc Nguyen Ba completed his PhD in Theoretical Physics from University of Science, Vietnam National University, Hanoi. Now he is Senior Lecturer of Tantrao University, Tuyenquang province, Vietnam, and he had also Leader of a strong group in the field of theoretical physics at the University of Tantrao and some other Universities. His fields of study are mainly related to X-Ray Absorption Fine Structure (XAFS) spectra theory and other fields of solid theory. He has published more than 50 scientific articles in both prestigious national and international journals.

PUBLIC INTEREST STATEMENT

The extended X-ray absorption fine structure (EXAFS) spectroscopy is one of the powerful techniques for investigating structures of crystalline. The formalism for including anharmonic effects in EXAFS is often written through cumulant expansion approach. There are many methods that have been developed to study the temperature dependence of EXAFS cumulants. However, no theoretical calculations have been done to predict the dependence of cumulants and thermodynamic parameters on temperature with the effects of pressure in EXAFS spectra. It requires the more accurate interatomic interaction form for metallic systems such as the many-body embedded-atom potentials. The purpose of this work is to investigate the dependence of cumulants and thermodynamic parameters on temperature with effects of pressure in EXAFS spectra of crystals. Anharmonic correlated Einstein model has been applied for compound of copper and silver with 72% ratio through the interatomic potential which has been derived by the Morse effective potential.

1. Introduction

Extended X-ray absorption fine structure (EXAFS) spectroscopy has developed into a powerful probe of atomic structure and the high-temperature thermodynamics of substances due to anharmonicity (Iwasawa et al., 2017; Rehr, 2000). Numerous methods have been developed to investigate how temperature affects the EXAFS cumulants, such as path-integral effective-potential theory (Yokoyama, 1999), the statistical moment method (V. v. Hung et al., 2010), the ratio method (Bunker, 1983), the Debye model (Beni & Platzman, 1976), the Einstein model (Frenkel & Rehr, 1993), and the anharmonic correlated Einstein model (ACEM) (N. v. Hung & Rehr, 1997). Several groups have applied ACEM theory to EXAFS to study how the thermodynamic properties depend on temperature with the effect of the material doping ratio (DR) (Duc et al., 2017; Hung et al., 2015; Kraut & Stern, 2000; Nafi et al., 2013). However, no reports to date have discussed how the thermodynamic parameters and the Debye–Waller factor (DWF) depend on temperature and pressure for Cu, Ag, and their intermetallic alloy CuAg72. A CuAg alloy contains the elements Cu and Ag, with the Ag atoms referred to as the substitution atoms and the Cu atoms referred to as the host atoms. CuAg72 has a ratio of 72% Ag and 28% Cu (±1%) and is also known as *CuSil* or *UNS* P0772 (note: *CuSil* should not be confused with *Cusil-ABA*, which has the composition 63.0% Ag, 35.25% Cu, and 1.75% Ti). It is an eutectic alloy and is used primarily for vacuum brazing (Nafi et al., 2013).

Herein, we use EXAFS theory (N. v. Hung & Rehr, 1997) to investigate how the DWF depends on temperature at high pressure. We also investigate thermodynamic parameters such as (i) the effective spring constant, (ii) the thermal expansion coefficient, (iii) the anharmonic factor, and (iv) the Einstein frequency and temperature and how they depend on temperature at ambient pressure for CuAg72.

2. Formalism

EXAFS is usually derived by using the cumulant-expansion approach, which contains the second cumulant σ^2 corresponding to the parallel mean-square relative displacement (MSRD) (Bunker, 1983). The second cumulant—often called the DWF—is an important factor in EXAFS analysis because the thermal lattice vibrations and high pressure strongly influence the EXAFS amplitudes through the function $e^{-2\sigma^2k^2}$(Duc et al., 2018; Rehr, 2000). For simplicity, the temperature and pressure dependences of the DWF are denoted as $\sigma^2(T)$ and $\sigma^2(p)$, respectively. One way to investigate how temperature and pressure affect the EXAFS cumulant is to combine ACEM with EXAFS (Hung, 2014; N. v. Hung & Rehr, 1997), which gives results that are consistent with experiments. ACEM uses the anharmonic effective interaction potential under pressure p, and the interatomic distance x is supplemented by $\delta r(p)$ to give

$$V_E(x,p) \approx \frac{1}{2}k_{eff}(x\delta r(p))^2 + k_{3eff}(x\delta r(p))^3 + k_{4eff}(x\delta r(p))^4 + \ldots \quad (1)$$

where k_{eff} is the effective spring constant, $k_{3\text{eff}}$ and $k_{4\text{eff}}$ are the effective cubic and quartic anharmonic parameters, respectively, which cause the asymmetry in the pair-distribution function, $\delta r(p) = r(p) - r(0)$ is the pressure-induced change in the interatomic distance, $x = r - r_0$ is the instantaneous bond length between atoms from the equilibrium location, r is the spontaneous bond length between absorbing and backscattering atoms, and r_0 is the equilibrium value of r. ACEM is determined by the vibration of single pairs of atoms, with M_1 and M_2 being the masses of the absorber and backscattering atoms, respectively. The oscillations of the absorber and backscattering atoms depend on their neighbors, so the interaction potential in Equation (1) is written in the form of an anharmonic effective interaction potential under ambient pressure, namely

$$V_E(x,p) = V(x,p) + \sum_{i=1,2}\sum_{j\neq i} V\left(\frac{\mu}{M_i}x\delta r(p)\hat{R}_{12}.\hat{R}_{ij}\right) \quad (2)$$

In Equation (2), $V(x, p)$ is the interaction potential between absorbing and backscattering atoms, the sum i is over absorber (i = 1) and backscattering (i = 2) atoms, and the sum j is over all nearest

neighbors whose contributions are described by the term $V(x, p)$ excluding the absorber and backscattering atoms themselves. Furthermore, M_i is the atomic mass of atom i, μ is the reduced atomic mass, namely $\mu = M_1M_2/(M_1 + M_2)$, and $\hat{R}$ is the unit vector for the bond between atoms i and j. Therefore, this effective pair potential describes not only the interaction between absorber and backscattering atoms but also how the nearest-neighbor atoms affect such interactions, which is the difference between the effective potential used in this work and the single-pair potential (Tranquada & Ingalls, 1997) or single-bond potential (Frenkel & Rehr, 1993), which consider only each pair of immediate-neighbor atoms [i.e., only $V(x)$] without considering the remaining terms on the right-hand side of Equation (2). The atomic vibration is calculated using a quantum statistical approach with an approximate anharmonic vibration in which the system Hamiltonian includes a harmonic term H_0 with respect to the equilibrium at a given temperature plus an anharmonic perturbation, namely

$$H = H_0 + V_E(a) + \delta V_E(a) \tag{3}$$

Here, the interaction potential $V_E(a)$ and anharmonic perturbation $\delta V_E(a)$ are

$$V_E(a) = k_{eff}a^2/2 + k_{3eff}a^3, \delta V_E(a) = (k_{eff} + 3k_{3eff}a^2)y + k_{3eff}y^2,$$

where a is the thermal expansion coefficient with $a = \langle x \rangle,\ y = x - a,\ \langle y \rangle = 0$. Equation (3) leads to the ACEM interactive potential

$$V_E = V_E(a) + k_{eff}y^2 + \delta V_E(y) \tag{4}$$

which is an anharmonic potential of Morse pairs and is appropriate for approximating the structure of cubic crystals. The Morse anharmonic potential is

$$V(r) = D\left(e^{-2\alpha(r-r_0)} - 2e^{-\alpha(r-r_0)}\right) = D\left(e^{-2\alpha x} - 2e^{-\alpha x}\right) \tag{5}$$

where $D(eV) = -V(r_0)$ is the dissociation energy and α_{12} ($Å^{-1}$) is the width of the potential. We expand Equation (5) in x to obtain the third-order term that describes approximately the cubic structure of doped crystals. When considering only crystals with orderly doping, we also assume that the lattice is not corrupted, and we designate Cu as the host atom with indicator 1 and Ag as the substituted atom with indicator 2. ACEM uses the Morse anharmonic pair potential to describe the pair interaction between atoms, namely

$$V_E(p) = D_{12}(e^{-2\alpha_{12}x\delta r(p)} - 2e^{-\alpha_{12}x\delta r(p)}) \approx D_{12}\left(-1 + \alpha_{12}^2(x\delta r(p))^2 - \alpha_{12}^3(x\delta r(p))^3 + \ldots\right) \tag{6}$$

For simplicity, we approximate the parameters of the Morse potential in Equation (6) at a given temperature by $D_{12} = c_1D_1 + c_2D_2, \quad \alpha_{12} = \sqrt{(D_1\alpha_1^2 + D_2\alpha_2^2)/(D_1 + D_2)},$ where $c_1,\ c_2$ are the doping ratios (%) of the intermetallic alloys. We calculate the sums in the second term of Equation (2) and compare the results with the terms of Equations (1) and (6) to obtain the effective force constant $k_{eff}(x, p) = \mu\omega_E^2(x, p) = 5D_{12}\alpha_{12}^2$ of the effective anharmonic potential. At ambient pressure, the effective force constant is $k_{eff}^0 = 23D_{12}\alpha_{12}^2/4$.

To derive analytical expressions for the cumulants, we use the perturbation theory (Duc et al., 2018; Hung, 2014). Atomic vibrations are quantized as phonons, and the phonon–phonon interaction leads to anharmonicity, with the phonon vibration frequency taking the form

$$\omega(x, p) = 2\sqrt{k_{eff}^0/\mu_{12}}|\sin(qa_0/2)|, \quad |q \le \pi/a_0| \tag{7}$$

where a_0 is the lattice constant at temperature T, and q is the phonon wave number. The correlated Einstein frequency and temperature at ambient pressure are, respectively

$$\omega_E^0 = 2\sqrt{k_{eff}^0/\mu_{12}}, \theta_E^0 = \hbar\omega_E^0/k_B \tag{8}$$

Using quantum thermodynamic perturbation theory (Hung et al., 2015) and Equations (1), (2), and (8), we obtain the first three EXAFS cumulants as functions of the ambient pressure and temperature. For the first cumulant or net thermal expansion, we have

$$\sigma^{(1)}(p,T)=\sigma_0^{(1)}(p)\frac{(1+z(p,T))}{(1-z(p,T))}=\frac{3\hbar\omega_E^0}{40D_{12}\alpha_{12}}\frac{(1+z(p,T))}{(1-z(p,T))},\sigma_0^{(1)}(p)=\frac{3\hbar\omega_E^0}{40D_{12}\alpha_{12}} \tag{9}$$

for the second cumulant or the DWF we have

$$\sigma^{(2)}(p,T)=\sigma_0^{2}(p)\frac{(1+z(p,T))}{(1-z(p,T))}=\frac{\hbar\omega_E^0}{10D_{12}\alpha_{12}^2}\frac{(1+z(p,T))}{(1-z(p,T))},\sigma_0^{2}(p)=\frac{\hbar\omega_E^0}{10D_{12}\alpha_{12}^2} \tag{10}$$

and for the third cumulant we have

$$\sigma^{(3)}(p,T)=\sigma_0^{(3)}(p)\frac{\left(1+10z(p,T)+(z(p,T))^2\right)}{(1-z(p,T))^2}=\frac{3\hbar^2\left(\omega_E^0\right)^2}{200D_{12}^2\alpha_{12}^3}\frac{\left(1+10z(p,T)+(z(p,T))^2\right)}{(1-z(p,T))^2} \tag{11}$$

$$\sigma_0^{(3)}(p)=\frac{3\hbar^2\left(\omega_E^0\right)^2}{200D_{12}^2\alpha_{12}^3}.$$

We also obtain the thermal expansion coefficient α_T and the anharmonic factor $\beta(T,p)$ as functions of ambient pressure and temperature as

$$\alpha(p,T)=\frac{3k_B}{20D_{12}\alpha_{12}r}\frac{z(p,T)\ln\left(z(p,T)\right)^2}{(1-z(p,T))^2},\alpha_0(p,T)=\frac{3k_B}{20D_{12}\alpha_{12}r}, \tag{12}$$

$$\beta(p,T)=\frac{9\eta k_BT}{16D_{12}}\left[1+\frac{3k_BT}{8D_{12}R\alpha_{12}}\left(1+\frac{3k_BT}{8D_{12}R\alpha_{12}}\right)\right],\eta=\frac{2z(p,T)}{1+z(p,T)}. \tag{13}$$

The second cumulant σ^2 contributes to the anharmonic EXAFS amplitude, while $\sigma^{(1)}$ and $\sigma^{(3)}$ contribute to the phase shift of the EXAFS due to anharmonicity. Note that $\sigma^{(1)}$, $\sigma^{(3)}$, and $\alpha(p,T)$ contain the anharmonicity parameter k_{3eff} and exist only when this parameter is included, which is why $\sigma^{(1)}$, $\sigma^{(3)}$, and $\alpha(p,T)$ must be considered when calculating the anharmonic effects in EXAFS. Under ambient pressure, the factor β is proportional to the temperature and inversely proportional to the shell radius, which is consistent with the anharmonicity obtained in experimental research into catalysis (Clausen et al., 1993), and R is considered as the particle radius. In Equations (9)–(13), $z(p,T)=\exp\left(-\theta_E^0/T\right)$ is the heat and pressure function, which describes how the cumulants, the thermal expansion coefficient, and the anharmonic factor depend on the absolute temperature T and pressure applied to the intermetallic alloy.

3. Results and discussion

For Cu-Cu and Ag-Ag pure metals and the alloy CuAg72, Table 1 gives the calculated and experimental (Benassi, 2018) parameters of the Morse potential, D_{12} and α_{12}, respectively. Substituting the parameters D_{12} and α_{12} from Table 1 into Equation (8), with the Boltzmann constant

Table 1. Parameters of Morse potential for pure metals and their intermetallic alloy

Crystal	D_{12}(eV)	$D_{12}^{expt.}$(eV)	α_{12}Å^{-1}	$\alpha_{12}^{Exp.}$Å^{-1}
Cu-Cu	0.3429	0.3528	1.3588	1.4072
Ag-Ag	0.3323	0.3253	1.3690	1.3535
CuAg72	0.3381	–	1.3634	–

Table 2. Effective parameters describing anharmonicity

Crystal	$k_{eff}(\text{eVA}^2)$	$k_{eff}^{Expt.}(\text{eVA}^2)$	$k_{eff}^0(\text{eVA}^2)$	$\omega_E(10^{13}Hz)$	$\omega_E^0(10^{13}Hz)$	$\theta_E(K)$	$\theta_E^0(K)$
Cu-Cu	3.1655	3.4931	3.6403	3.0889	4.7710	236	364
Ag-Ag	3.1139	2.9797	3.5810	3.3933	3.6585	176	279
CuAg72	3.1423	–	3.6138	2.6874	4.3623	207	333

$k_B = 8.617 \times 10^{-5}\text{eVK}^{-1}$ and Planck's constant $\hbar = 6.5822 \times 10^{-16}eV.s$, we calculate the values of the Einstein frequency and temperature at ambient pressures up to 14 GPa for Cu-Cu, Ag-Ag, and CuAg72 crystals and hence deduce the local force constant. Table 2 lists the results, where $k_{eff}^{expt.}$ is the local force constant deduced from the results of Okube and Yoshiasa (2001) and Okube et al. (2003).

Inserting the thermodynamic parameters from Tables 1 and 2 into Equations (1) and (9)–(13) gives the effective anharmonic potential $V_E(x,p)$ as a function of the departure x from equilibrium bond length and ambient pressure (see Figure 1). The cumulants $\sigma^{(n)}(n)$ depend on the absolute temperature T and are influenced by pressure up to 14 GPa (see Figures 2–5). Figure 6 shows the thermal expansion coefficient $\alpha(T,p)$ as a function of absolute temperature T and pressure, and Figure 7 shows the anharmonic factor $\beta(T,p)$.

Figure 1 compares the calculated anharmonic effective Morse potential $V_E(x,p)$ for CuAg72 at 300 K and 0.1 MPa (solid lines) with results from the theories of Okube et al. (2003) (dotted curve) and Okube and Yoshiasa (2001) (dashed curve). The curves calculated for the Morse potential align closely with those obtained from the theories of Okube and Yoshiasa (2001) and Okube et al. (2003), indicating that the coefficients k_{eff}, k_{3eff}, and k_{eff}^0 calculated by using the ACEM (given in Table 2) are in reasonable agreement with measurements and the calculations of Okube et al. for CuAg72.

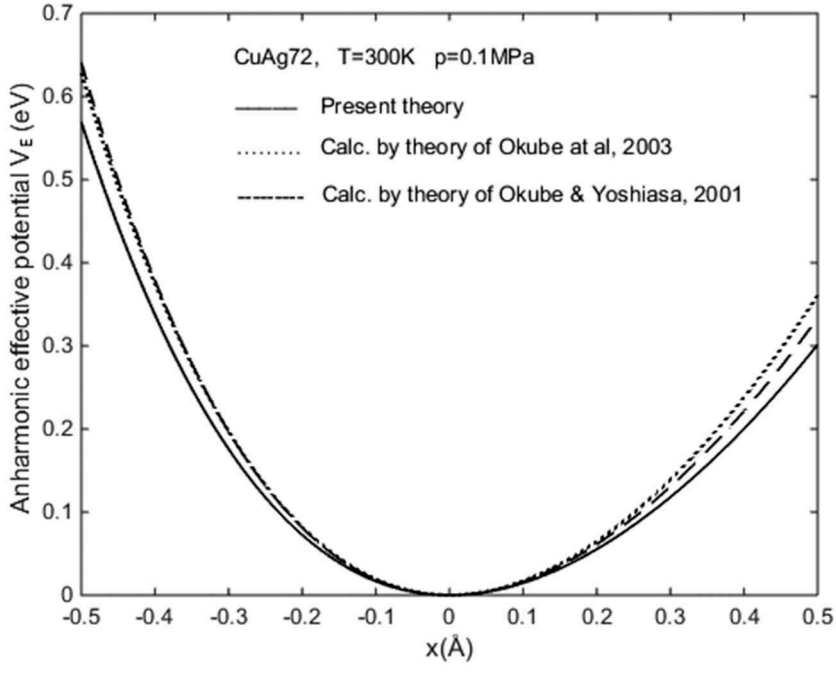

Figure 1. Anharmonic effective potential $V_E(x, p)$.

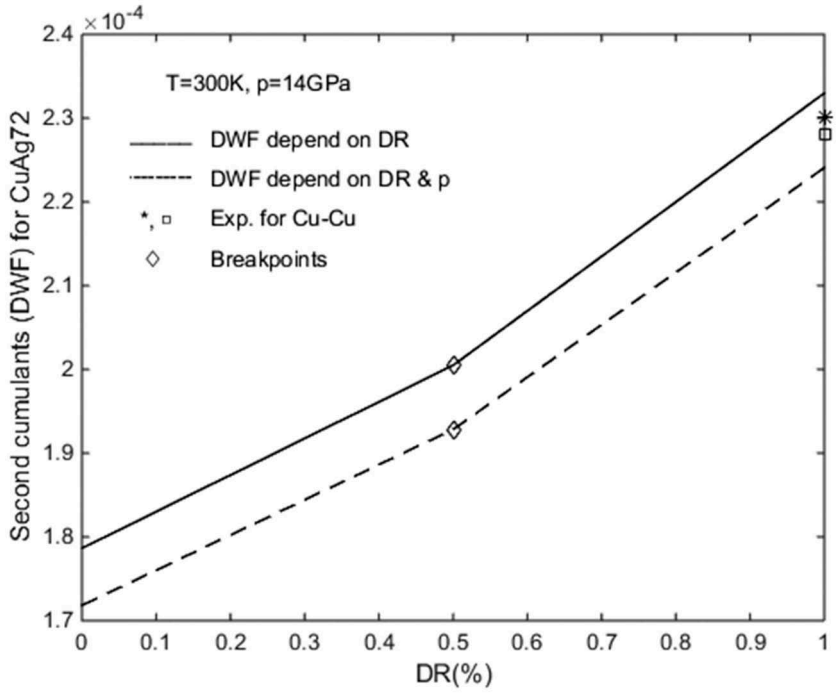

Figure 2. Second cumulant σ^2 (DWF) for CuAg72 as a function of doping ratio (DR).

Figure 2 shows our calculation of the second cumulant or DWF as a function of the DR at 300 K and an ambient pressure of 14 GPa for the crystalline alloy CuAg72. These results illustrate that for DRs of 0–50% and 50–100%, the DWF varies linearly with the DR (with different slopes in each range). For DR = 100% (i.e., where the Ag content is 0% and the Cu content is 100%), the calculated values are in good agreement with experimental values determined at 300 K (see symbols *, □) (Hung et al., 2002; N. v. Hung & Duc, 1999, 2000). However, there are breakpoints in the lines at 50% DR, which means that we do not have ordered atoms at DR = 50%. Thus, the Cu-Ag alloy does not form an ordered phase at the molar composition of 1:1 (i.e., the alloy CuAg50 does not exist), and this result is consistent with the findings of Kraut and Stern (2000). As the ambient pressure increases, the DWF decreases: with 0% Ag, 100% Cu, and 101 kPa (i.e., normal atmospheric pressure), we have DWF = 0.2330 Å^2 (for 14 GPa, DWF = 0.2241 Å^2); with 100% Ag, 0% Cu, and 101 kPa, we have DWF = 0.1796 Å^2 (for 14 GPa, DWF = 0.1718 Å^2). At the breakpoints, we have DWF = 0.2005 Å^2 and 0.1928 Å^2 at 101 kPa and 14 GPa, respectively. Thus, increasing the ambient pressure decreases the EXAFS amplitude by reducing the atomic MSRD that characterizes the EXAFS DWF.

Figure 3 shows the first cumulant $\sigma^{(1)}$ as a function of temperature at the pressure of 14 GPa for Cu, Ag, and CuAg72. At approximately the zero point with 101 kPa and 14 GPa ambient pressure, we have $\sigma^{(1)} = 0.0027$ Å and $\sigma^{(1)} = 0.0047$ Å, respectively; at 700 K, we have $\sigma^{(1)} = 0.0184$ Å and $\sigma^{(1)} = 0.0201$ Å, respectively. Thus, as the pressure increases, the first cumulant also increases, but at low temperature, it deviates more, meaning that the pressure causing the net thermal expansion is more pronounced at low temperatures.

Figure 4 shows the second cumulant or DWF as a function of absolute temperature with the effects of ambient pressure for Cu-Cu, Ag-Ag, and CuAg72 and compares these results with experimental results (Hung et al., 2002; N. v. Hung & Duc, 1999). The calculated values for the first cumulant (Figure 3) and the DWF (Figure 4) for different DRs at the pressure of 14 GPa are proportional to temperature from around 100 K and above.

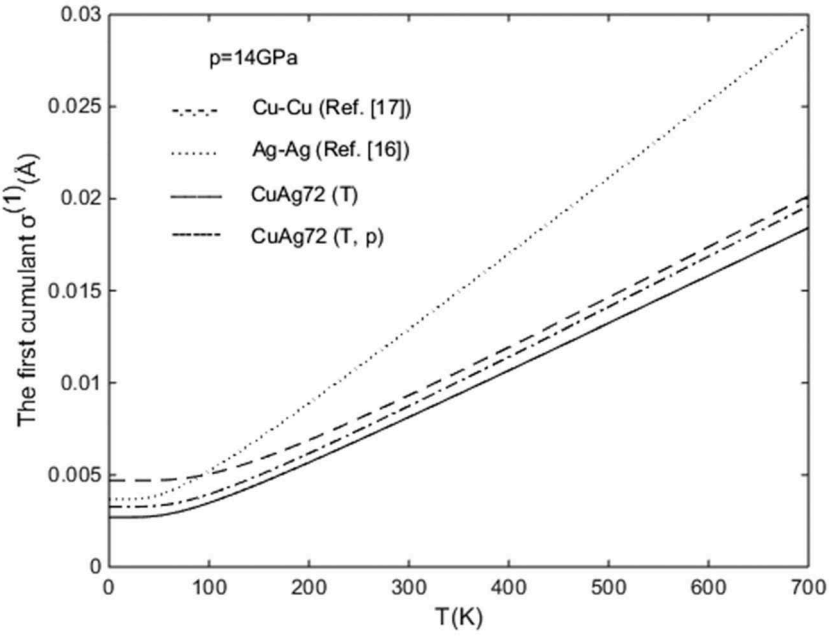

Figure 3. First cumulant for Cu, Ag, and CuAg72.

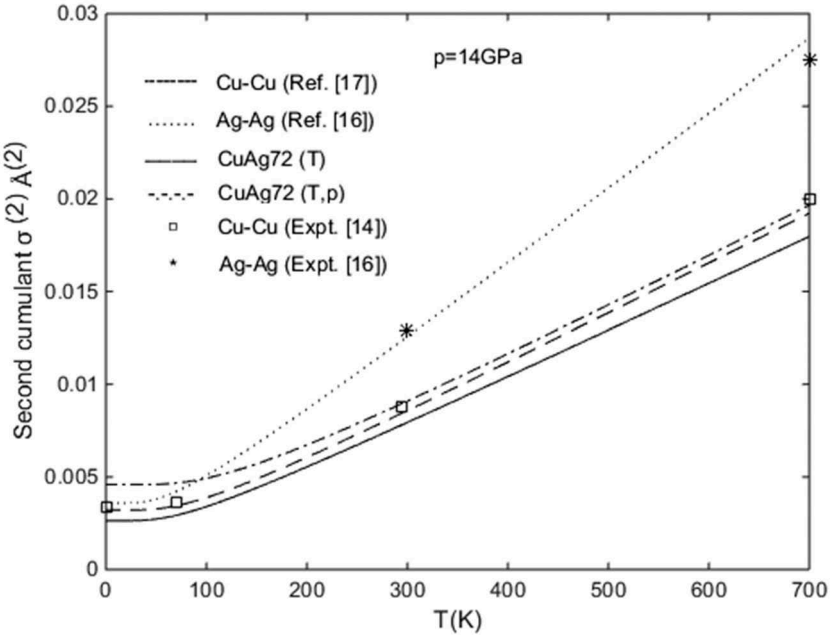

Figure 4. Second cumulant (DWF) for Cu, Ag, and CuAg72.

Consider the change in the second cumulant (DWF) for different temperatures. At approximately 0 K, the DWF increases from $\sigma^{(2)}$= 0.0026 Å^2 to $\sigma^{(2)}$= 0.0046 Å^2 as the pressure increases from normal atmospheric pressure up to 14 GPa. At 700 K, the DWF increases from $\sigma^{(2)}$= 0.018 Å^2 to $\sigma^{(2)}$= 0.0197 Å^2 as the pressure increases from normal atmospheric pressure up to 14 GPa. At low temperatures, the DWF changes more than it does at high temperatures because the change in ambient pressure from 101 kPa to 14 GPa causes a greater MSRD of the atoms (or second cumulant $\sigma^{(2)}$). Furthermore, Figure 4 shows that from room temperature upward (approximately 300 K), the DWF remains almost constant as the ambient pressure increases, so the ambient pressure has a stronger effect at low temperatures.

Figure 5. Third cumulant for Cu, Ag, and CuAg72.

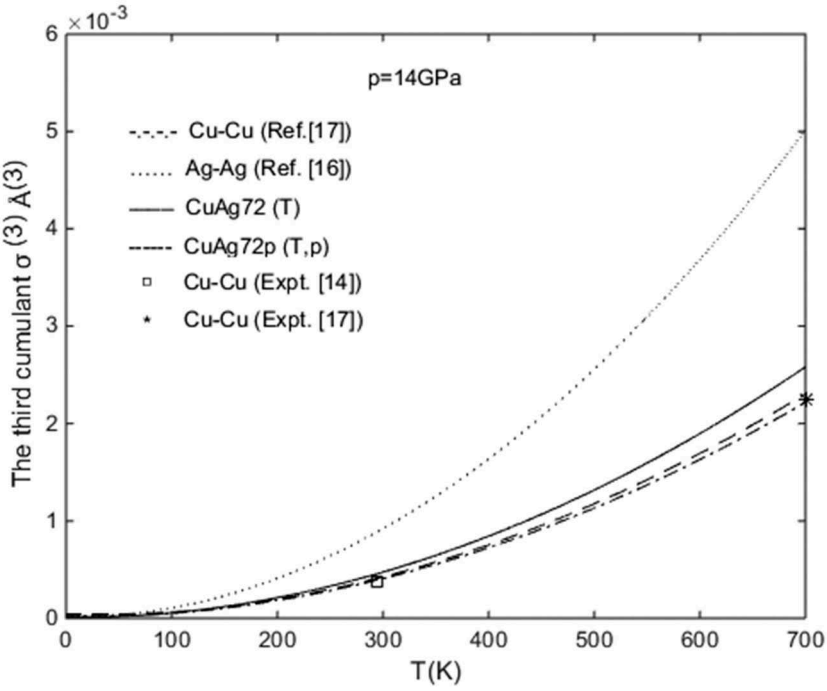

Figure 5 shows the third cumulant $\sigma^{(3)}$ for Cu-Cu, Ag-Ag, and CuAg72 as a function of absolute temperature and at normal atmospheric pressure (101 kPa) and at the pressure of 14 GPa. The calculated results for Cu-Cu and Ag-Ag are consistent with experimental results (Hung et al., 2002; N. v. Hung & Duc, 1999, 2000) at normal atmospheric pressure. At 0 K for both 101 kPa and 14 GPa, the third cumulant $\sigma^{(3)}\approx 0$, but as the temperature increases, $\sigma^{(3)}$ for CuAg72 decreases with pressure: at 700 K, we have $\sigma^{(3)}$= 0.0026 Å^3 at 101 kPa and 0.0023 Å^3 at 14 GPa. Thus, high ambient pressure reduces the asymmetry of the atomic interaction potential at higher temperatures.

The results shown in Figures 3–5 for CuAg72 at all pressures are very similar to the results for Cu-Cu, demonstrating the consistency between theoretical and experimental results. The calculated first three cumulants contain zero-point contributions at low temperatures, resulting from an asymmetry of the atomic interaction potential due to anharmonicity even at high pressure, which is consistent with established theories (Duc et al., 2018; Frenkel & Rehr, 1993; Rehr, 2000; N. v. Hung & Rehr, 1997).

Figure 6 shows the thermal expansion coefficient α_T for Cu-Cu, Ag-Ag, and CuAg72 as a function of absolute temperature with the effects of ambient pressure. The calculated results for Cu-Cu are consistent with experimental results (Hung et al., 2002) at normal atmospheric pressure; however, the result for CuAg72 is deflected from 70 to 400 K^{-1} when the ambient pressure is 14 GPa, which shows that because of the effect at high pressure, the thermal expansion coefficient α_T for CuAg72 is reduced significantly in the room-temperature range but changes very little when the temperature exceeds 700 K.

The graph of α_T has the form of the specific heat C_V, thus reflecting the fundamental principle of solid-state theory, which states that thermal expansion results from anharmonic effects and is proportional to the specific heat C_V (Duc et al., 2018). Our calculated values of α_T approach the constant value α_T^0 at high temperatures and vanish exponentially with θ_E/T at low temperatures, which is consistent with the results of previous research (N. v. Hung & Duc, 1999, 2000).

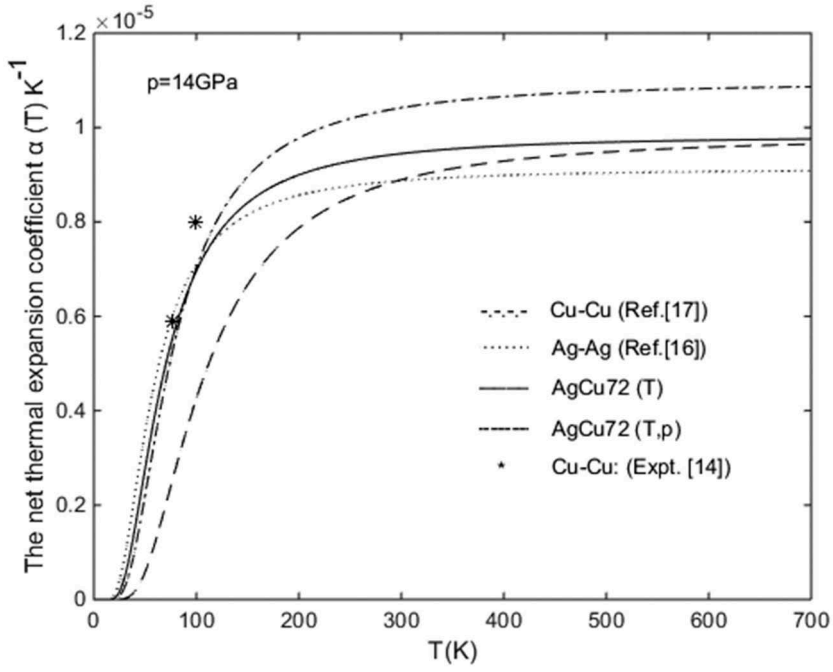

Figure 6. Net thermal expansion coefficient for Cu, Ag, and CuAg72.

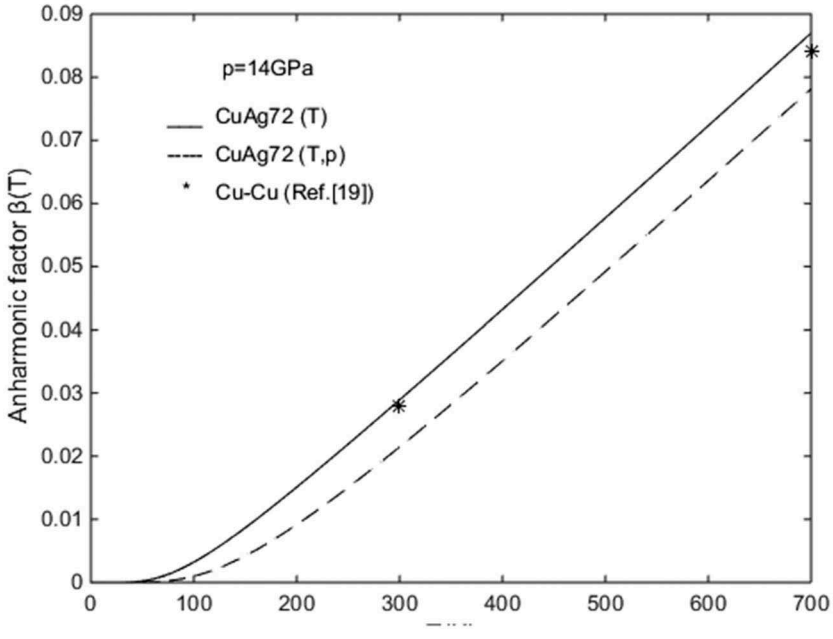

Figure 7. Anharmonic factor for Cu and CuAg72.

Figure 7 shows the anharmonic factor $\beta(T)$ as a function of absolute temperature and pressure for CuAg72. For both normal and high pressure (14 GPa), $\beta(T)$ is negligibly small at low temperature and increases strongly when the temperature exceeds 100 K. At normal atmospheric pressure, we have θ_E = 176 K for Ag, θ_E = 236 K for Cu, and θ_E = 207 K for CuAg72. At high pressure, we have θ_E^0 = 279 K for Ag, θ_E^0 = 364 K for Cu, and θ_E^0 = 333 K for CuAg72. The results shown in Figure 7 are consistent with experimental results (Hung et al., 2002), which demonstrates that our calculations for CuAg72 are appropriate for normal atmospheric pressure. At temperatures above 100 K with

increasing pressure, the anharmonic factor $\beta^0(T)$ is less than at normal pressure $\beta(T)$; in other words, $\beta^0(T)$= 0.3125$\beta(T)$ at 100 K, $\beta^0(T)$= 0.7439$\beta(T)$ at 300 K, and $\beta^0(T)$ = 0.898$\beta(T)$ at 700 K. Thus, the anharmonic factor describes the temperature dependence of the anharmonic EXAFS theory under the influence of high ambient pressure.

4. Conclusions

In this work, based on quantum statistical theory and by applying the effective ACEM to EXAFS spectra, we derive analytical expressions for the temperature dependence of the cumulants and thermodynamic parameters of crystalline Cu, Ag, and their alloy CuAg72 under the influence of pressures up to 14 GPa. The expressions for the second cumulant or DWF, the thermodynamic parameters, the effective force constant, and the correlated Einstein frequency and temperature for Cu, Ag, and CuAg72 agree with the known properties for these quantities. The expressions for calculations involving orderly doped crystals have forms similar to those for pure crystals.

Figures 1–7 show the cumulants and thermodynamic parameters for doped crystals as functions of absolute temperature and pressure. The calculated results are consistent with experimental results and other studies of Cu and Ag, and the results for CuAg72 are coherent. Thus, the method developed herein, which is based on applying the ACEM to EXAFS, is appropriate for calculating and analyzing the cumulant and thermodynamic properties of intermetallic alloys.

Funding

This research is funded by Vietnam National Foundation for Science and Technology Development (NAFOSTED) under grant number 103.01-2019.55

Author details

Nguyen Ba Duc[1]
E-mail: ducnb@daihoctantrao.edu.vn
[1] Faculty of Physics, Tan Trao University, Tuyen Quang, Viet Nam.

Citation information

Cite this article as: Investigation of temperature and pressure effects on thermodynamic parameters of intermetallic alloy in EXAFS, Nguyen Ba Duc, *Cogent Engineering* (2020), 7: 1759184.

References

Benassi, E. (2018). The zero point position in Morse's potential and accurate prediction of thermal expansion in metals. *Chemical Physics*, *515*, 323. https://doi.org/10.1016/j.chemphys.2018.09.005

Beni, G., & Platzman, P. M. (1976). Temperature and polarization dependence of extended x-ray absorption fine-structure spectra. *Physical Review B*, *14*(4), 1514. https://doi.org/10.1103/PhysRevB.14.1514

Bunker, G. (1983). Application of the ratio method of EXAFS analysis to disordered systems. *Nuclear Instruments and Methods in Physics Research*, *207*(3), 437. https://doi.org/10.1016/0167-5087(83)90655-5

Clausen, B. S., Grabæk, L., Topsoe, H., Hansen, L. B., Stoltze, P., Norskǿv, J. K., & Nielsen, O. H. (1993). A new procedure for particle size determination by EXAFS based on molecular dynamics simulations. *Journal of Catalysis*, *141*(2), 368. https://doi.org/10.1006/jcat.1993.1147

Duc, N. B., Hieu, H. K., Binh, N. T., & Nguyen, K. C. (2018). X-ray absorption fine structure: basic and applications. *Sciences and Technics Publishing House, Hanoi, Vietnam*, ISBN: 978-604-67-1107-0, pp 69, 158.

Duc, N. B., Tho, V. Q., Hung, N. V., Khoa, D. Q., & Hieu, H. K. (2017). Anharmonic effects of gold in extended X-ray absorption fine structure. *Vacuum*, *145*, 272. https://doi.org/10.1016/j.vacuum.2017.09.009

Frenkel, A. I., & Rehr, J. J. (1993). Thermal expansion and x-ray-absorption fine-structure cumulants. *Physical Review B*, *48*(1), 585. https://doi.org/10.1103/PhysRevB.48.585

Hung, N. V. (2014). Pressure-dependent anharmonic correlated Einstein model extended X-ray absorption fine structure Debye–Waller factors. *Journal of the Physical Society of Japan*, *83*(2), 024802. https://doi.org/10.7566/JPSJ.83.024802

Hung, N. V., & Duc, N. B. (1999). *Proceedings of the third international workshop on material science*. IWOM'S99. Ha Noi, Viet Nam

Hung, N. V., & Duc, N. B. (2000). Anharmonic-correlated Einstein model thermal expansion and XAFS cumulants of cubic crystals: Comparison with experiment and other theories. *Communications in Physics (ISSN: 0868-3166)*, *10*, 15.

Hung, N. V., Duc, N. B., & Frahm, R. R. (2002). A new anharmonic factor and EXAFS including anharmonic contributions. *Journal of the Physical Society of Japan*, *72*(5), 1254. https://doi.org/10.1143/JPSJ.72.1254

Hung, N. V., & Rehr, J. J. (1997). Anharmonic correlated Einstein-model Debye-Waller factors. *Physical Review B*, *56*(1), 43. https://doi.org/10.1103/PhysRevB.56.43

Hung, N. V., Trung, N. B., & Duc, N. B. (2015). Temperature Dependence of high-order Expanded XAFS Debye Waller Factors of Metallic Nickel Studied based on Anharmonic Correlated Debye Model.The *Journal of Materials Science Applications*, *1(2)*, 91. http://www.aascit.org/journal/jmsa

Hung, V. V., Hieu, H. K., & Masuda-Jindo, K. (2010). Study of EXAFS cumulants of crystals by the statistical moment method and anharmonic correlated Einstein model. *Computational Materials Science*, *49*, 5214. ISSN: 0927-0256

Iwasawa, Y., Asakura, K., & Tada, M. (2017). *XAFS techniques for catalysts, nanomaterials, and surfaces*. Springer International Publishing.

Kraut, J. C., & Stern, W. B. (2000). The density of gold-silver-copper alloys and its calculation from the

chemical composition. *Gold Bulletin*, *33*(2), 52. https://doi.org/10.1007/BF03216580

Nafi, A., Cheikh, M., Mercier, O., & Adhes, J. (2013). Identification of mechanical properties of CuSil-steel brazed structures joints: A numerical approach. *Journal of Adhesion Science and Technology*, *27*, 2705.ISSN: 0169-4243

Okube, M., & Yoshiasa, A. (2001). Anharmonic effective pair potentials of group VIII and Ib fcc metals. *Journal of Synchrotron Radiat*. *8*, 937.ISSN: 1600-5775

Okube, M., Yoshiasa, A., Ohtaka, O., & Katayama, Y. (2003). Anharmonicity of platinum under HP and HT. *High Pressure Research*, *23*(3), 247. https://doi.org/10.1080/0895795032000102423

Rehr, J. J. (2000). Theoretical approaches to x-ray absorption fine structure. *Reviews of Modern Physics*, *72*(3), 621. https://doi.org/10.1103/RevModPhys.72.621

Tranquada, J. M., & Ingalls, R. (1997). Extended x-ray—Absorption fine-structure study of anharmonicity in CuBr. *Physical Review B*, *28*(6), 3520. https://doi.org/10.1103/PhysRevB.28.3520

Yokoyama, T. (1999). Path-integral effective-potential theory for EXAFS cumulants compared with the second-order perturbation. *Journal of Synchrotron Radiation*, *6*(3), 323. https://doi.org/10.1107/S0909049599001521